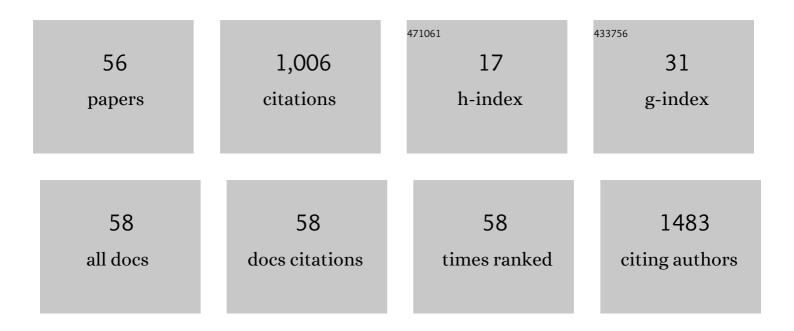
Tomofumi Takaya

List of Publications by Year in descending order

Source: https://exaly.com/author-pdf/371200/publications.pdf Version: 2024-02-01



#	Article	IF	CITATIONS
1	Main pulmonary artery compression by a giant aneurysm associated with a coronary-pulmonary artery fistula. European Heart Journal Cardiovascular Imaging, 2022, 23, e162-e162.	0.5	0
2	A large iatrogenic tearing of atrial septal defect after MitraClip implantation: a rare and cautionary complication during transcatheter edge-to-edge mitral valve repair. European Heart Journal - Case Reports, 2022, 6, ytac119.	0.3	0
3	Newly developed spontaneous echocardiographic contrast as a potential marker of intracardiac thrombus formation after a transcatheter edge-to-edge mitral valve repair. European Heart Journal - Case Reports, 2022, 6, ytac146.	0.3	0
4	Dark crescent sign: high-risk calcified coronary plaque detected by electrocardiogram-gated non-contrast computed tomography. European Heart Journal - Case Reports, 2022, 6, ytab519.	0.3	0
5	Single-Cell RNA Sequencing Reveals a Distinct Immune Landscape of Myeloid Cells in Coronary Culprit Plaques Causing Acute Coronary Syndrome. Circulation, 2022, 145, 1434-1436.	1.6	14
6	Utility of coronary orbital atherectomy with guideâ€extension system for distally located undilatable inâ€stent restenosis: A case report. Clinical Case Reports (discontinued), 2022, 10, e05798.	0.2	2
7	Combined therapy with excimer laser coronary atherectomy and intracoronary thrombolysis for the management of massive thrombi in coronary aneurysms of post-Kawasaki disease myocardial infarction. European Heart Journal - Case Reports, 2022, 6, ytac186.	0.3	1
8	ViperSlide-Induced Anaphylaxis. JACC: Cardiovascular Interventions, 2022, 15, e117-e118.	1.1	0
9	Histopathological findings of late-phase restenosis after directional coronary atherectomy with drug-coated balloon angioplasty: a case report. European Heart Journal - Case Reports, 2022, 6, .	0.3	0
10	Novel strategy for ostial left anterior descending artery acute myocardial infarction: Combined treatment with directional coronary atherectomy followed by drugâ€coated balloon angioplasty. Clinical Case Reports (discontinued), 2021, 9, 1095-1100.	0.2	1
11	Comparison of the 9-Month Intrastent Condition and 30-Month Clinical Outcomes After Resolute Zotarolimus-Eluting Stent Implantation Between Standard-Duration and 1-Month Dual Antiplatelet Therapy Followed by Prasugrel Monotherapy. Circulation Reports, 2021, 3, 55-65.	0.4	1
12	The impact of vildagliptin on the daily glucose profile and coronary plaque stability in impaired glucose tolerance patients with coronary artery disease: VOGUE—A multicenter randomized controlled trial. BMC Cardiovascular Disorders, 2021, 21, 92.	0.7	6
13	Posterior Reversible Encephalopathy Syndrome. JACC: Cardiovascular Interventions, 2021, 14, e73-e75.	1.1	0
14	Additional ablation effect of lowâ€speed rotational atherectomy following highâ€speed rotational atherectomy on early calcified inâ€stent restenosis: A case report. Clinical Case Reports (discontinued), 2021, 9, e04550.	0.2	0
15	Morphological Plaque Characteristics and Clinical Outcomes in Patients With Acute Coronary Syndrome and a Cancer History. Journal of the American Heart Association, 2021, 10, e020243.	1.6	5
16	Acute Coronary and Cerebral Emboli From a Pedunculated Ascending Aorta Thrombus. JACC: Case Reports, 2021, 3, 1194-1199.	0.3	2
17	In-stent restenosis due to delayed healing of abluminal bioresorbable polymer everolimus-eluting stent: insight from histopathological evaluation with directional coronary atherectomy. European Heart Journal - Case Reports, 2021, 5, ytab370.	0.3	2
18	Coronary Orbital Atherectomy at the Ostium of an Anomalous Right Coronary Artery. JACC: Cardiovascular Interventions, 2020, 13, 2937-2939.	1.1	1

Томоғимі Такауа

#	Article	IF	CITATIONS
19	Favorable early vessel healing after everolimus-eluting stent implantation: 3-, 6-, and 12-month follow-up of optical coherence tomography. Journal of Cardiology, 2018, 72, 193-199.	0.8	6
20	The association between wedging of the aorta and cardiac structural anatomy as revealed using multidetectorâ€row computed tomography. Journal of Anatomy, 2017, 231, 110-120.	0.9	17
21	The impact of serum trans fatty acids concentration on plaque vulnerability in patients with coronary artery disease: Assessment via optical coherence tomography. Atherosclerosis, 2017, 265, 312-317.	0.4	18
22	Effects of daily glucose fluctuations on the healing response to everolimus-eluting stent implantation as assessed using continuous glucose monitoring and optical coherence tomography. Cardiovascular Diabetology, 2016, 15, 79.	2.7	36
23	High perfusion pressure as a predictor of reperfusion pulmonary injury after balloon pulmonary angioplasty for chronic thromboembolic pulmonary hypertension. IJC Heart and Vasculature, 2016, 11, 1-6.	0.6	12
24	Bending of the aortic valvar leaflet causing severe aortic regurgitation in a patient with osteogenesis imperfecta. European Heart Journal Cardiovascular Imaging, 2016, 17, 708-708.	0.5	7
25	Clinical cardiac structural anatomy reconstructed within the cardiac contour using multidetectorâ€row computed tomography: Atrial septum and ventricular septum. Clinical Anatomy, 2016, 29, 342-352.	1.5	16
26	Clinical cardiac structural anatomy reconstructed within the cardiac contour using multidetectorâ€row computed tomography: Left ventricular outflow tract. Clinical Anatomy, 2016, 29, 353-363.	1.5	15
27	Clinical cardiac structural anatomy reconstructed within the cardiac contour using multidetectorâ€row computed tomography: The arrangement and location of the cardiac valves. Clinical Anatomy, 2016, 29, 364-370.	1.5	9
28	Impact of residual platelet reactivity under clopidogrel treatment for lesions and the clinical outcome after drug-eluting stent implantation in patients with hemodialysis. Journal of Cardiology, 2016, 67, 531-537.	0.8	9
29	Serum phosphate is an independent predictor of the total aortic calcification volume in non-hemodialysis patients undergoing cardiovascular surgery. Journal of Cardiology, 2016, 68, 308-315.	0.8	2
30	Association between daily glucose fluctuation and coronary plaque properties in patients receiving adequate lipid-lowering therapy assessed by continuous glucose monitoring and optical coherence tomography. Cardiovascular Diabetology, 2015, 14, 78.	2.7	40
31	Clinical structural anatomy of the inferior pyramidal space reconstructed from the living heart: Threeâ€dimensional visualization using multidetectorâ€row computed tomography. Clinical Anatomy, 2015, 28, 878-887.	1.5	20
32	Optimal angulations for obtaining an en face view of each coronary aortic sinus and the interventricular septum: Correlative anatomy around the left ventricular outflow tract. Clinical Anatomy, 2015, 28, 494-505.	1.5	16
33	Effect of Daily Glucose Fluctuation on Coronary Plaque Vulnerability in Patients Pre-Treated With Lipid-Lowering Therapy. JACC: Cardiovascular Interventions, 2015, 8, 800-811.	1.1	64
34	Serial Optical Coherence Tomography Evaluation at 6, 12, and 24 Months After Biolimus A9-Eluting Biodegradable Polymer-Coated Stent Implantation. Canadian Journal of Cardiology, 2015, 31, 980-988.	0.8	14
35	Three-dimensional quantification and visualization of aortic calcification by multidetector-row computed tomography: A simple approach using a volume-rendering method. Atherosclerosis, 2015, 239, 622-628.	0.4	19
36	Reconstruction of an Extracardiac Aortocoronary Collateral and Simulation of Selective Angiography With Multidetector-Row Computed Tomography. Circulation, 2015, 131, e476-9.	1.6	2

Томоғимі Такауа

#	Article	IF	CITATIONS
37	Clinical Structural Anatomy of the Inferior Pyramidal Space Reconstructed Within the Cardiac Contour Using Multidetectorâ€Row Computed Tomography. Journal of Cardiovascular Electrophysiology, 2015, 26, 705-712.	0.8	22
38	Impact of cytochrome P450 2C19 loss-of-function polymorphism on intra-stent thrombi and lesion outcome after everolimus-eluting stent implantation compared to that after first-generation drug-eluting stent implantational Journal of Cardiology, 2015, 179, 476-483.	0.8	9
39	Association between the rotation and threeâ€dimensional tortuosity of the proximal ascending aorta. Clinical Anatomy, 2014, 27, 1200-1211.	1.5	14
40	Analysis by Optical Coherence Tomography of Long-term Arterial Healing After Implantation of Different Types ofÂStents. Canadian Journal of Cardiology, 2014, 30, 904-911.	0.8	7
41	Favorable Vessel Healing After Nobori Biolimus A9-Eluting Stent Implantation. Circulation Journal, 2014, 78, 1882-1890.	0.7	17
42	Qualitative and Quantitative Assessment of Stent Restenosis by Optical Coherence Tomography. Circulation Journal, 2013, 77, 652-660.	0.7	35
43	Coronary artery bypass grafting for the occlusion of left main trunk and right coronary artery guided by computed tomographic angiography. European Heart Journal Cardiovascular Imaging, 2012, 13, 800-800.	0.5	Ο
44	The usefulness of transesophageal echocardiographic observation during chemotherapy for cardiac metastasis of non-Hodgkin lymphoma complicated with left ventricular diastolic collapse. Journal of Cardiology, 2009, 53, 447-452.	0.8	8
45	Torsades de Pointes with QT prolongation related to donepezil use. Journal of Cardiology, 2009, 54, 507-511.	0.8	56
46	Plasma Tetrahydrobiopterin/Dihydrobiopterin Ratio A Possible Marker of Endothelial Dysfunction. Circulation Journal, 2009, 73, 955-962.	0.7	47
47	Atherosclerotic plaque imaging using phase-contrast X-ray computed tomography. American Journal of Physiology - Heart and Circulatory Physiology, 2008, 294, H1094-H1100.	1.5	46
48	Mitral regurgitation resulting from the consecutive multiple perforations by infective endocarditis mimicking the isolated anterior mitral cleft. Journal of Cardiology, 2008, 52, 159-162.	0.8	2
49	Augmentation of Vascular Remodeling by Uncoupled Endothelial Nitric Oxide Synthase in a Mouse Model of Diabetes Mellitus. Arteriosclerosis, Thrombosis, and Vascular Biology, 2008, 28, 1068-1076.	1.1	50
50	Beneficial Effects of Exogenous Tetrahydrobiopterin on Left Ventricular Remodeling After Myocardial Infarction in Rats The Possible Role of Oxidative Stress Caused by Uncoupled Endothelial Nitric Oxide Synthase. Circulation Journal, 2008, 72, 1512-1519.	0.7	47
51	A Specific Role for eNOS-Derived Reactive Oxygen Species in Atherosclerosis Progression. Arteriosclerosis, Thrombosis, and Vascular Biology, 2007, 27, 1632-1637.	1.1	79
52	Xenogenic macrophage immunization reduces atherosclerosis in apolipoprotein E knockout mice. American Journal of Physiology - Cell Physiology, 2007, 293, C865-C873.	2.1	4
53	Local Overexpression of Toll-Like Receptors at the Vessel Wall Induces Atherosclerotic Lesion Formation. Arteriosclerosis, Thrombosis, and Vascular Biology, 2007, 27, 2384-2391.	1.1	62
54	Angiotensin II type 1 receptor blocker telmisartan suppresses superoxide production and reduces atherosclerotic lesion formation in apolipoprotein E-deficient mice. Atherosclerosis, 2006, 186, 402-410.	0.4	110

#	Article	IF	CITATIONS
55	An X-Ray Diffraction Study on Mouse Cardiac Cross-Bridge Function In Vivo: Effects of Adrenergic β-Stimulation. Biophysical Journal, 2006, 90, 1723-1728.	0.2	26
56	Xenogenic smooth muscle cell immunization reduces neointimal formation in balloon-injured rabbit carotid arteries. Cardiovascular Research, 2005, 68, 249-258.	1.8	8